

Natural Convection in a Periodically Heated Slot

M. Z. Hossain¹ and J. M. Floryan²

¹Department of Mechanical Engineering
Bangladesh University of Engineering and Technology (BUET)
Dhaka-1000, Bangladesh

²Department of Mechanical and Materials Engineering
The University of Western Ontario, London, Ontario, N6A5B9, Canada

Abstract

Heat transfer resulting from the natural convection in a fluid layer contained in an infinite horizontal slot bounded by solid walls and subject to a spatially periodic heating at the lower wall has been investigated. The heating produces sinusoidal temperature variations along one horizontal direction characterized by the wave number α with the amplitude expressed in terms of a suitably defined Rayleigh number Ra_p . The maximum heat transfer takes place for the heating with the wave numbers $\alpha=0(1)$ as this leads to the most intense convection. The strength of convection decreases proportionally to α for small heating wave numbers, resulting in the heat transfer being dominated by periodic conduction with the Nusselt number decreasing proportionally to α^2 . When α becomes large, the convection is confined to a thin layer adjacent to the lower wall with its strength decreasing proportionally to α^{-3} , with the temperature field above the convection layer losing dependence on the horizontal direction.

Introduction

Fluid systems exposed to spatially distributed heating patterns are ubiquitous in nature. Illustrative examples include convection in atmospheric boundary layer as surfaces of different colours heat up at different rates, e.g., patterns of forests/lakes in rural environments and patterns of roofs/streets in urban environments, convection induced by patterns of heat sources, e.g., systems of localized fires, computer chips, thermal patterning in micro-fluidic devices for biological applications, and many others. The characteristic property of such systems is the existence of horizontal gradients of buoyancy force which drive convection regardless of the intensity of the heating. This is in contrast with the well known Rayleigh-Bénard (RB) convection [1,2] where the heating must meet certain critical conditions in order to set the fluid into a motion. In spite of the obvious relevance, convection resulting from spatially distributed heating has not attracted much attention. The existing results are limited to simple sinusoidal temperature distributions. Analysis of arbitrary heating patterns is yet to be attempted. There have been a number of studies dealing with convection in slots formed by isothermal walls fitted with spatially-periodic grooves [3-5].

To our best knowledge, Kelly and Pal [6] were the first to study convection resulting from the sinusoidal heating using asymptotic methods in the long wavelength limit. Yoo and Kim [7] used Direct Numerical Simulation (DNS) to investigate convection with the heating wavelength comparable to the channel height

and demonstrated existence of a steady convection replaced by a sequence of bifurcations as the heating intensity increased.

As evidenced by the above discussion, the knowledge of even the fundamental features of convection driven by a periodic heating is very limited. The objective of this analysis is therefore to determine the basic characteristics of the heat transfer process in a simple reference system consisting of an infinite horizontal layer subject to heating from below. We shall focus attention on the simplest heating pattern represented by one Fourier mode and investigate system response in the complete range of the heating wave numbers α .

Problem formulation

Consider fluid contained in a slot between two parallel plane plates extending to $\pm\infty$ in the x-direction and placed at a distance $2h$ apart each other with the gravitational acceleration g acting in the negative y-direction, as shown in Fig.1. The upper plate is kept isothermal while the lower plate is subject to a periodic heating resulting in the temperatures of the lower (θ_L) and upper (θ_U) walls in the form

$$\theta_L(x) = 1/2 \cos(\alpha x), \quad \theta_U(x) = 0 \quad (1)$$

where $\lambda=2\pi/\alpha$ is the wavelength of the heating, θ denotes the relative temperature scaled with the amplitude of the peak to peak temperature variations along the wall T_d , i.e., $\theta = (T - T_U)/T_d$, T denotes the absolute temperature and T_U denotes the temperature of the upper wall. The fluid is incompressible, Newtonian, with thermal conductivity k , specific heat c , thermal diffusivity $\kappa=k/\rho c$, kinematic viscosity ν , dynamic viscosity μ , thermal expansion coefficient Γ and variations of the density ρ that follow the Boussinesq approximation.

The temperature field is represented as a sum of the conductive field Θ and the convective field θ . Two temperature scales are used, i.e., T_d defined above as the conductive temperature scale and $T_v = T_d \nu / \kappa$ as the convective temperature scale. $T_v/T_d = Pr$ where $Pr = \nu / \kappa$ stands for the Prandtl number. Half of distance between the plates h is used as the length scale, $U_v = \nu/h$ is used as the (convective) velocity scale and $P_v = \rho U_v^2$ is used as the (dynamic) pressure scale.

The complete dimensionless temperature θ_{tot} is scaled with the convective scale and takes the form

$$\theta_{\text{tot}}(x, y) = \text{Pr}^{-1}\Theta(x, y) + \theta(x, y) \quad (2)$$

where the conductive temperature Θ is determined analytically, has the form

$$\Theta(x, y) = \frac{1}{4} \left[-\frac{\sinh(\alpha y)}{\sinh(\alpha)} + \frac{\cosh(\alpha y)}{\cosh(\alpha)} \right] \cos(\alpha x) = \Theta^{(1)}(y)e^{i\alpha x} + \Theta^{(-1)}(y)e^{-i\alpha x} \quad (3)$$

and does not generate net heat flow across the slot. The maximum of θ_{tot} in this scaling is always $(2\text{Pr})^{-1}$. The dimensionless field equations describing convection have the form

$$\mathbf{u} \frac{\partial \mathbf{u}}{\partial x} + \mathbf{v} \frac{\partial \mathbf{u}}{\partial y} = -\frac{\partial p}{\partial x} + \nabla^2 \mathbf{u}, \quad (4a)$$

$$\mathbf{u} \frac{\partial \mathbf{v}}{\partial x} + \mathbf{v} \frac{\partial \mathbf{v}}{\partial y} = -\frac{\partial p}{\partial y} + \nabla^2 \mathbf{v} + \text{Ra}_p \theta + \text{Ra}_p \text{Pr}^{-1} \Theta, \quad (4b)$$

$$\text{Pr} \left(\mathbf{u} \frac{\partial \theta}{\partial x} + \mathbf{v} \frac{\partial \theta}{\partial y} \right) + \mathbf{u} \frac{\partial \Theta}{\partial x} + \mathbf{v} \frac{\partial \Theta}{\partial y} = \nabla^2 \theta, \quad (4c)$$

$$\frac{\partial \mathbf{u}}{\partial x} + \frac{\partial \mathbf{v}}{\partial y} = 0, \quad (4d)$$

where $\mathbf{v} = (u, v)$ denotes the velocity vector, p stands for the pressure, $\text{Ra}_p = g\Gamma h^3 T_d / \nu \kappa$ is the Rayleigh number and ∇^2 denotes the Laplace operator. The boundary conditions take the form

$$\mathbf{u}(\pm 1) = 0, \quad \mathbf{v}(\pm 1) = 0, \quad \theta(\pm 1) = 0. \quad (5)$$

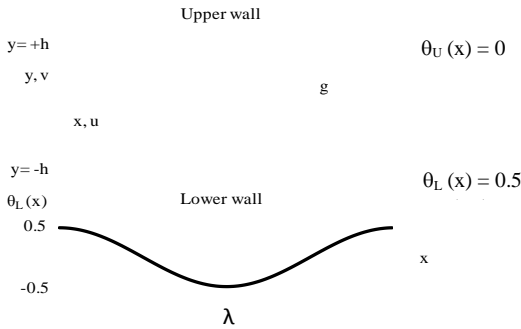


Figure 1. Sketch of the system configuration.

Method of solution

Stream function $\psi(x, y)$ is introduced in the usual manner, i.e., $\mathbf{u} = \partial \psi / \partial y$, $\mathbf{v} = -\partial \psi / \partial x$, and pressure is eliminated resulting in the following form of governing equations

$$\nabla^4 \psi - \text{Ra}_p \frac{\partial \theta}{\partial x} - \text{Ra}_p \text{Pr}^{-1} \frac{\partial \Theta}{\partial x} = \mathbf{N}_\psi, \quad (6a)$$

$$\nabla^2 \theta = \text{Pr} \mathbf{N}_\theta + \mathbf{N}_\Theta \quad (6b)$$

where ∇^4 denotes the biharmonic operator, terms involving products and nonlinearities are expressed as

$$\mathbf{N}_\psi = \frac{\partial}{\partial y} \left(\frac{\partial}{\partial x} \langle \mathbf{u}\mathbf{u} \rangle + \frac{\partial}{\partial y} \langle \mathbf{u}\mathbf{v} \rangle \right) - \frac{\partial}{\partial x} \left(\frac{\partial}{\partial x} \langle \mathbf{u}\mathbf{v} \rangle + \frac{\partial}{\partial y} \langle \mathbf{v}\mathbf{v} \rangle \right),$$

$$\mathbf{N}_\theta = \frac{\partial}{\partial x} \langle \mathbf{u}\theta \rangle + \frac{\partial}{\partial y} \langle \mathbf{v}\theta \rangle, \quad \mathbf{N}_\Theta = \frac{\partial}{\partial x} \langle \mathbf{u}\Theta \rangle + \frac{\partial}{\partial y} \langle \mathbf{v}\Theta \rangle$$

and $\langle \dots \rangle$ denotes products. The solution is assumed in the form of Fourier expansions, i.e.,

$$\psi(x, y) = \sum_{n=-\infty}^{n=+\infty} \varphi^{(n)}(y) e^{in\alpha x}, \quad \theta(x, y) = \sum_{n=-\infty}^{n=+\infty} \varphi^{(n)}(y) e^{in\alpha x},$$

$$\mathbf{u}(x, y) = \sum_{n=-\infty}^{n=+\infty} \mathbf{u}^{(n)}(y) e^{in\alpha x}, \quad \mathbf{v}(x, y) = \sum_{n=-\infty}^{n=+\infty} \mathbf{v}^{(n)}(y) e^{in\alpha x} \quad (7)$$

where $\mathbf{u}^{(n)} = D\varphi^{(n)}$ and $\mathbf{v}^{(n)} = -in\alpha\varphi^{(n)}$. The nonlinear and product terms are also expressed in terms of Fourier expansions in the form

$$\langle \mathbf{u}\mathbf{u} \rangle(x, y) = \sum_{n=-\infty}^{n=+\infty} \langle \mathbf{u}\mathbf{u} \rangle^{(n)}(y) e^{in\alpha x},$$

$$\langle \mathbf{u}\mathbf{v} \rangle(x, y) = \sum_{n=-\infty}^{n=+\infty} \langle \mathbf{u}\mathbf{v} \rangle^{(n)}(y) e^{in\alpha x},$$

$$\langle \mathbf{v}\mathbf{v} \rangle(x, y) = \sum_{n=-\infty}^{n=+\infty} \langle \mathbf{v}\mathbf{v} \rangle^{(n)}(y) e^{in\alpha x}, \quad (8)$$

$$\langle \mathbf{u}\theta \rangle(x, y) = \sum_{n=-\infty}^{n=+\infty} \langle \mathbf{u}\theta \rangle^{(n)}(y) e^{in\alpha x},$$

$$\langle \mathbf{v}\theta \rangle(x, y) = \sum_{n=-\infty}^{n=+\infty} \langle \mathbf{v}\theta \rangle^{(n)}(y) e^{in\alpha x},$$

$$\langle \mathbf{u}\Theta \rangle(x, y) = \sum_{n=-\infty}^{n=+\infty} \langle \mathbf{u}\Theta \rangle^{(n)}(y) e^{in\alpha x}.$$

Substitution of (7)-(8) into (6) and separation of Fourier components result in the following system of ordinary differential equations for the modal functions

$$D_n^2 \varphi^{(n)} - in\alpha \text{Ra}_p \varphi^{(n)} = in\alpha \text{Ra}_p \text{Pr}^{-1} \Theta^{(n)} + \mathbf{N}_\psi^{(n)}, \quad (9a)$$

$$D_n \varphi^{(n)} = \mathbf{N}_\Theta^{(n)} + \text{Pr} \mathbf{N}_\theta^{(n)} \quad (9b)$$

where $-\infty < n < +\infty$, $D = d/dy$, $D^2 = d^2/dy^2$, $D_n = D^2 - n^2\alpha^2$,

$$\mathbf{N}_\theta^{(n)} = in\alpha \langle \mathbf{u}\theta \rangle^{(n)} + D \langle \mathbf{v}\theta \rangle^{(n)},$$

$$\mathbf{N}_\Theta^{(n)} = in\alpha \langle \mathbf{u}\Theta \rangle^{(n)} + D \langle \mathbf{v}\Theta \rangle^{(n)},$$

$$\mathbf{N}_\psi^{(n)} = in\alpha D \langle \mathbf{u}\mathbf{u} \rangle^{(n)} + D^2 \langle \mathbf{u}\mathbf{v} \rangle^{(n)} + in^2 \alpha^2 \langle \mathbf{u}\mathbf{v} \rangle^{(n)} - in\alpha D \langle \mathbf{v}\mathbf{v} \rangle^{(n)}$$

and $\Theta^{(n)} \neq 0$ for $n = \pm 1$. The unknown linear terms have been placed on the left hand side, and the nonlinear and product terms have been placed on the right hand side. The required boundary conditions have the form

$$\varphi^{(n)}(\pm 1)=0, \quad D\varphi^{(n)}(\pm 1)=0, \quad \phi^{(n)}(\pm 1)=0. \quad (10a-c)$$

For the purpose of numerical solution, expansions (7)-(8) have been truncated after N_M modes. The discretization method uses Chebyshev Collocation technique based on the Gauss-Chebyshev-Lobatto points. The resulting nonlinear algebraic system is solved using an iterative technique combined with under-relaxation in the form $\Phi_{j+1} = \Phi_j + RF(\Phi_{\text{comp}} - \Phi_j)$ where $\Phi = \{\varphi^{(n)}, \phi^{(n)}\}$ is the vector of unknowns, Φ_{comp} denotes the current solution, Φ_j denotes the previous solution, Φ_{j+1} stands for the accepted value of the next iteration and RF denotes the relaxation factor. The solution process starts with solution of (9)-(10) with the RHS terms assumed to be zero. Afterwards, a new approximation of the RHS terms is computed on the basis of the most recent approximation of the velocity and temperature fields and the system (9)-(10) is resolved with the new approximation of the RHS. This process is continued, with the update of the RHS terms taking place after each iteration, until a convergence criterion in the form $\max(|\Phi_{\text{comp}} - \Phi_j|) < \text{TOL}$ is satisfied. TOL denotes difference between solutions obtained in two consecutive iterations and its value set at 10^{-8} was found to be sufficient in most of the computations. The number of collocation points and the number of Fourier modes used in the solution were selected through numerical experiments so that the flow quantities of interest were determined with at least six digits accuracy.

The evaluation of the RHS terms requires evaluation of products of two Fourier series. It is more efficient to evaluate these product in the physical rather than in the Fourier space [8]. The required flow quantities, i.e., u , v , θ , were computed in the physical space on a suitable grid based on the collocation points in the y -direction and a uniformly distributed set of points in the x -direction, and the required products were evaluated at the grid points. The Fast Fourier Transform (FFT) algorithm was used to express these products in terms of Fourier expansions (8). The aliasing error was controlled using "padding" [8], i.e., using of a discrete FFT transform with N_p rather than N_M points, where $N_p \geq 3N_M / 2$. Zeros were added for the additional Fourier modes as required.

The primary quantity of interest is the net heat transfer between the walls which can be expressed in terms of the Nusselt number Nu based on the conductive temperature scale in the form

$$Nu = \frac{Pr}{\lambda} \int_0^\lambda \left(-\frac{d\theta}{dy} \right)_{y=-1} dx = -Pr \left. \frac{d\phi^{(0)}}{dy} \right|_{y=-1}. \quad (11)$$

Results

The topology of the velocity field is made of pairs of counter-rotating rolls with the flow directed upwards above the hot spots. The strength of convection can be measured using the maximum of the stream function ψ_{max} . It can be shown that this strength decreases proportionally to α when $\alpha \rightarrow 0$, i.e.

$$\psi_{\text{max}} = \alpha Ra_p Pr^{-1} \left[3 + (21/5)^{1/2} \right] \left[15(21/5)^{1/2} - 4 \right] + O(\alpha^3), \quad (12)$$

as the horizontal gradients of the buoyancy force driving this motion decrease with α (Fig.2). Convective temperature

modifications decrease proportionally to α^2 resulting in the dominance of the conductive component. As a result, the net heat flow between the walls decreases proportionally to α^2 when $\alpha \rightarrow 0$ (Fig.3), i.e.

$$Nu = \frac{1}{1400} \alpha^2 Ra_p \left(1 - \frac{92}{135} \alpha^2 \right) + O(\alpha^6) \quad (13)$$

The strength of convection also decreases when $\alpha \rightarrow \infty$. It can be shown (see Fig.2) that

$$\psi_{\text{max}} = 0.0331267 Ra_p Pr^{-1} \alpha^{-3}, \quad (14)$$

which leads to a decrease of the Nusselt number

$$Nu = 0.00192 Ra_p \alpha^{-3}. \quad (15)$$

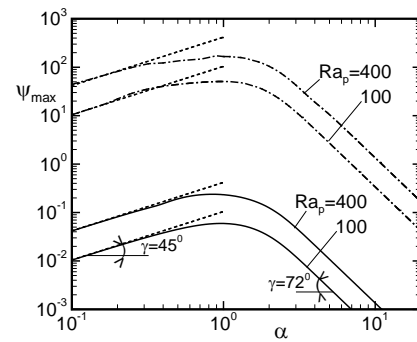


Figure 2. Variations of the maximum of the stream function ψ_{max} as a function of the heating wave number α for $Ra_p=100, 400$. Solid and dash-dot lines are for the Prandtl numbers $Pr=10$ and 0.01 , respectively, dotted lines denote the corresponding asymptotes. $\psi_{\text{max}} \sim \alpha^1$ for $\alpha \rightarrow 0$, $\psi_{\text{max}} \sim \alpha^{-3}$ for $\alpha \rightarrow \infty$.

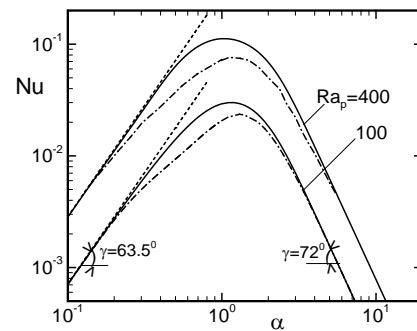


Figure 3. Variations of the Nusselt number Nu as a function of the heating wave number α for $Ra_p=100, 400$. Solid and dash-dot lines are for the Prandtl numbers $Pr=10$ and 0.01 , respectively, dotted lines denote the corresponding asymptotes. $Nu \sim \alpha^2$ for $\alpha \rightarrow 0$, $Nu \sim \alpha^{-3}$ for $\alpha \rightarrow \infty$.

Analysis of results presented in Fig. 2 demonstrates that the heating pattern corresponding to $\alpha \approx 1$ leads to the most intense motion regardless of values of Ra_p and Pr . The most effective heat transfer corresponds to the same pattern of heating, as illustrated in Fig.3.

Figure 4 illustrates variations of the strength of convection as a function of the heating intensity. It can be seen that this strength

increases proportionally to Ra_p while, at the same time, the heating wave number that leads to the most intense convection decreases. Figure 5 illustrates the resulting changes in the Nusselt number.

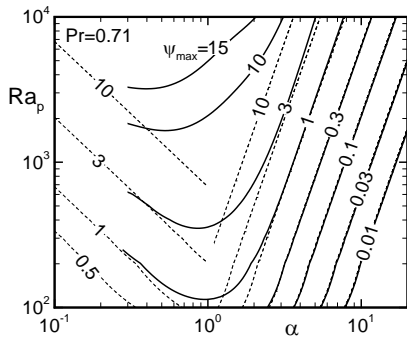


Figure 4. Variations of the roll strength ψ_{max} as a function of the heating wave number α and the Rayleigh number Ra_p . Dotted lines describe asymptotes.

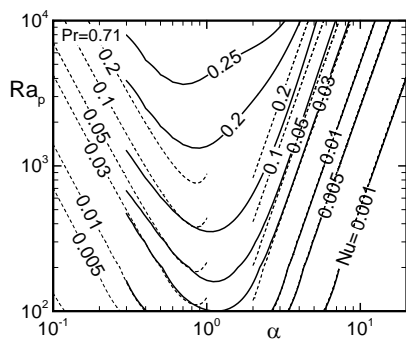


Figure 5. Variations of the Nusselt number Nu as a function of the heating wave number α and the Rayleigh number Ra_p . Dotted lines describe asymptotes.

Conclusions

Analysis of the natural convection heat transfer in an infinitely long slot bounded by solid plates has been carried out. The external heating results in a periodic temperature distribution in a selected horizontal direction along the lower wall. The heating pattern is characterized by the wave number α and its intensity is expressed in terms of the Rayleigh number Ra_p based on the amplitude of the temperature variations along the lower wall. The heating produces horizontal gradients of buoyancy force that

drive convection regardless of the magnitude of the heating. The resulting motion has the form of pairs of counter-rotating rolls with the fluid moving upwards above the hot spots. The flow topology remains unchanged in the whole range of α . It is shown that the most intense convection and the maximum heat transfer occur for $\alpha \approx 1$ regardless of Ra_p . When $\alpha \rightarrow 0$ (long wavelength heating), the intensity of convection decreases, the temperature field becomes dominated by conduction associated with periodic heating and the net heat flow between the walls decreases proportionally to α^2 . When $\alpha \rightarrow \infty$ (short wavelength heating), the intensity of convection also decreases, the convection becomes confined to a thin layer attached to the lower wall (convection layer), a zone of pure conduction appears above the convection layer, spatial temperature modulation is confined only to the convection layer and the heat flow between the walls is driven by vertical conduction through the conduction layer.

Acknowledgments

This work has been carried out with the support of NSERC of Canada.

References

- [1] Bénard, H., Les tourbillons cellulaires dans une nappe liquide, *Revue Gen. Sci. Pure Appl.*, **11**, 1900, 1261-1271.
- [2] Rayleigh, J.W.S., 1916, On convection currents in a horizontal layer of fluid, when the higher temperature is on the under side, *Phil. Mag.*, **32**, 1916, 529-546.
- [3] Sparrow, E.M., Charmchi, M., Heat Transfer and Fluid Flow Characteristics of Spanwise-Periodic Corrugated Ducts, *Int. J. Heat Mass Transfer*, **23**, 1980, 471-481.
- [4] Asako, Y., Nakamura, H., Faghri, M., Heat Transfer and Pressure Drop Characteristics in a Corrugated Duct with Rounded Corners, *Int. J. Heat Mass Transfer*, **31**, 1988, 1237-1245.
- [5] Ligrani, P.M., Oliveira, M.M., Blaskovich, T., Comparison of Heat Transfer Augmentation Techniques, *AIAA J.*, **41**, 2003, 337-362.
- [6] Kelly, R., E. & Pal, D., 1976, Thermal convection induced between non-uniformly heated horizontal surfaces. *Proc. 1976 Heat Transfer and Fluid Mech. Inst.*, 1-17, Stanford University Press.
- [7] Yoo, J.S., Two-dimensional convection in a horizontal fluid layer with spatially periodic boundary conditions, *Fluid Dynamics Research*, **7**, 1991, 181-200.
- [8] Canuto, C., Hussaini, M.Y., Quarteroni, A., Zang, T.A., 1996, *Spectral Methods*, Springer.